Journal of Hydrology 542 (2016) 450–462

Contents lists available at ScienceDirect

Journal of Hydrology

journal homepage: www.elsevier.com/locate/jhydrol

Research papers

Spatial interpolation of river channel topography using the shortest temporal distance

Yanjun Zhang [a,*], Cuiling Xian [a], Huajin Chen [b], Michael L. Grieneisen [b], Jiaming Liu [a], Minghua Zhang [b]

[a] State Key Laboratory of Water Resources & Hydropower Engineering Science, Wuhan University, Wuhan, China
[b] Department of Land, Air and Water Resources, University of California Davis, CA, USA

ARTICLE INFO

Article history:
Received 11 October 2015
Received in revised form 16 August 2016
Accepted 7 September 2016
Available online 14 September 2016
This manuscript was handled by Peter K. Kitanidis, Editor-in-Chief, with the assistance of Roseanna M. Neupauer, Associate Editor

Keywords:
Shortest temporal distance
Modified shortest temporal distance
Locally varying anisotropy
River channel topography
Interpolation

ABSTRACT

It is difficult to interpolate river channel topography due to complex anisotropy. As the anisotropy is often caused by river flow, especially the hydrodynamic and transport mechanisms, it is reasonable to incorporate flow velocity into topography interpolator for decreasing the effect of anisotropy. In this study, two new distance metrics defined as the time taken by water flow to travel between two locations are developed, and replace the spatial distance metric or Euclidean distance that is currently used to interpolate topography. One is a shortest temporal distance (STD) metric. The temporal distance (TD) of a path between two nodes is calculated by spatial distance divided by the tangent component of flow velocity along the path, and the STD is searched using the Dijkstra algorithm in all possible paths between two nodes. The other is a modified shortest temporal distance (MSTD) metric in which both the tangent and normal components of flow velocity were combined. They are used to construct the methods for the interpolation of river channel topography. The proposed methods are used to generate the topography of Wuhan Section of Changjiang River and compared with Universal Kriging (UK) and Inverse Distance Weighting (IDW). The results clearly showed that the STD and MSTD based on flow velocity were reliable spatial interpolators. The MSTD, followed by the STD, presents improvement in prediction accuracy relative to both UK and IDW.

1. Introduction

Topographic data of rivers play an important role in modeling and simulating the flow (Harvey and Bencala, 1993), the transport of sediments and pollutants (Marzadri et al., 2014; Wildhaber et al., 2014), the stream-aquifer interactions (Shope et al., 2012), and the hydrologic response of a basin (Mejia and Reed, 2011). These data are typically obtained by conventional ground-based surveys based on transverse profiles, also known as cross-sections, at locations selected to capture salient features of the topography (Legleiter and Kyriakidis, 2008). The data obtained are often sparse and discrete, and the interpolation and extrapolation must be implemented for satisfying the requirements of modeling and simulation. Inverse Distance Weighting (IDW), Spline, Kriging and their derivatives are the most common spatial prediction techniques (Merwade, 2009; Schwendel et al., 2012), but the strong anisotropy that exists in the topography of river channels makes it difficult to predict the topography using those methods (Legleiter and Kyriakidis, 2008).

For the anisotropy of river channel topography, one possible solution is to remove certain trends from the original data. Merwade (2009) presented a method for calculating the trend of river bathymetry by transforming the Cartesian coordinates to body-fitted coordinates based on the meandering nature of river along the centerline or river bank. This bathymetric trend was then removed before interpolation using the typical IDW, Kriging and Spline methods. Legleiter and Kyriakidis (2008) developed a suite of Kriging algorithms that were appropriate for various combinations of channel morphology features based on the coordinate transformation from Cartesian coordinates to a channel-centered system. Additionally, Rivest et al. (2012) presented a Kriging method improved by a coordinate transformation based on natural flow coordinates and alternative flow coordinates for solute concentration maps prediction, which provided better mapping than Kriging on Cartesian coordinates for a 3-D problem.

The other main method is to find a non-Euclidean distance to replace the Euclidean distance which is typically used by default in spatial interpolators. Gardner et al. (2003) predicted the stream

* Corresponding author.
E-mail address: zhangyj1015@hotmail.com (Y. Zhang).

http://dx.doi.org/10.1016/j.jhydrol.2016.09.022
0022-1694/

Fig. 1. Wuhan section of the Changjiang River, China.

temperature by comparing three different geostatistical metrics in Kriging: the shortest path, the distances along the stream network, and a modified network system in which the distances were weighted by stream order. Hoef et al. (2006) developed models that incorporated flow and stream distance by using spatial moving averages, and showed that models using flow might be more appropriate than models that only use stream distance. Babak and Deutsch (2008) provided an approach to integrate statistical control into IDW, which could replace the integrated Euclidean distance in IDW, and presented its potential use in the case of variogram misspecification. Boisvert and Deutsch (2011b) presented a new method for incorporating locally varying anisotropy in Kriging and IDW, in which the shortest anisotropic path distance (SPD) between locations was used. Boisvert and Deutsch (2011a) applied this technique in modeling locally varying anisotropy of CO_2 emissions in the United States, and the results showed an improvement in cross validation. Based on the SPD, Li et al. (2014) also developed a method which used shortest wind-field path distance (SWPD) to replace the Euclidean distance in IDW. This method generated estimation surfaces for the particulate matter concentrations in the urban study area.

For all of the approaches implemented in the above studies, the spatial distance was used in the interpolator technique. However, for the river systems, anisotropy is often the result of hydrodynamic or transport mechanisms, and the principal axes of the anisotropy are determined by the direction of flow (Kitanidis, 1997). Therefore, the flow velocity may be introduced into topography interpolator for decreasing the effect of anisotropy. This study developed a technique for solving the anisotropy of river channel topography using the temporal distance metrics defined as the time cost that flow travelled between two nodes. The temporal distance metrics were presented to replace the spatial distances that are often used in regular spatial interpolators. The corresponding interpolation methods were developed, and used to predict the topography of a river channel in the study area. In addition, comparisons were made among the performances of the STD, MSTD, Universal Kriging (UK) and Inverse Distance Weighting (IDW).

2. Study area

Topography samples of the channel were collected at the Wuhan Section of Changjiang River at Wuhan city, Hubei Province, China (Fig. 1). The section is located at the center of Changjiang River downstream of Three Gorges Dam, which is an area of great concern to government agencies and the public. The fine-scale and accurate river channel topography data is critical for a variety of research projects in this important river system. The length of the section is 42 km with the mean width 1.8 km. The substrate type is mainly the sandy and silty sediments. The expected resolution of topography is 50 × 50 m, and a 440 × 346 grid was generated to cover the study area, which yielded 22176 valid nodes within the river channel. Fig. 2 shows the elevations of the 1183 samples (mean 9.8 m and standard deviation 6.53 m), which were surveyed by the Changjiang Waterway Bureau (CWB) in April 2000.

3. Methodology

3.1. The shortest temporal distance method (STD)

In most situations, the default spatial distance (SD) between a pair of nodes is calculated by Eq. (1).

$$S_{AB} = \sqrt{\Delta x^2 + \Delta y^2} \quad (1)$$

where S_{AB} is the spatial distance between nodes A and B (m); Δx and Δy are the horizontal and vertical spatial distances between nodes A and B (m).

For the rivers, the flow is the critical factor causing channel topographic change, which is obviously distributed along the thalweg and streamline and is not identical in all spatial directions. The anisotropy is often the result of hydrodynamic or transport mechanisms, and the principal axes of the anisotropy are determined by the direction of flow (Kitanidis, 1997). In this study, a temporal distance is defined as the time cost that the flow travelled between

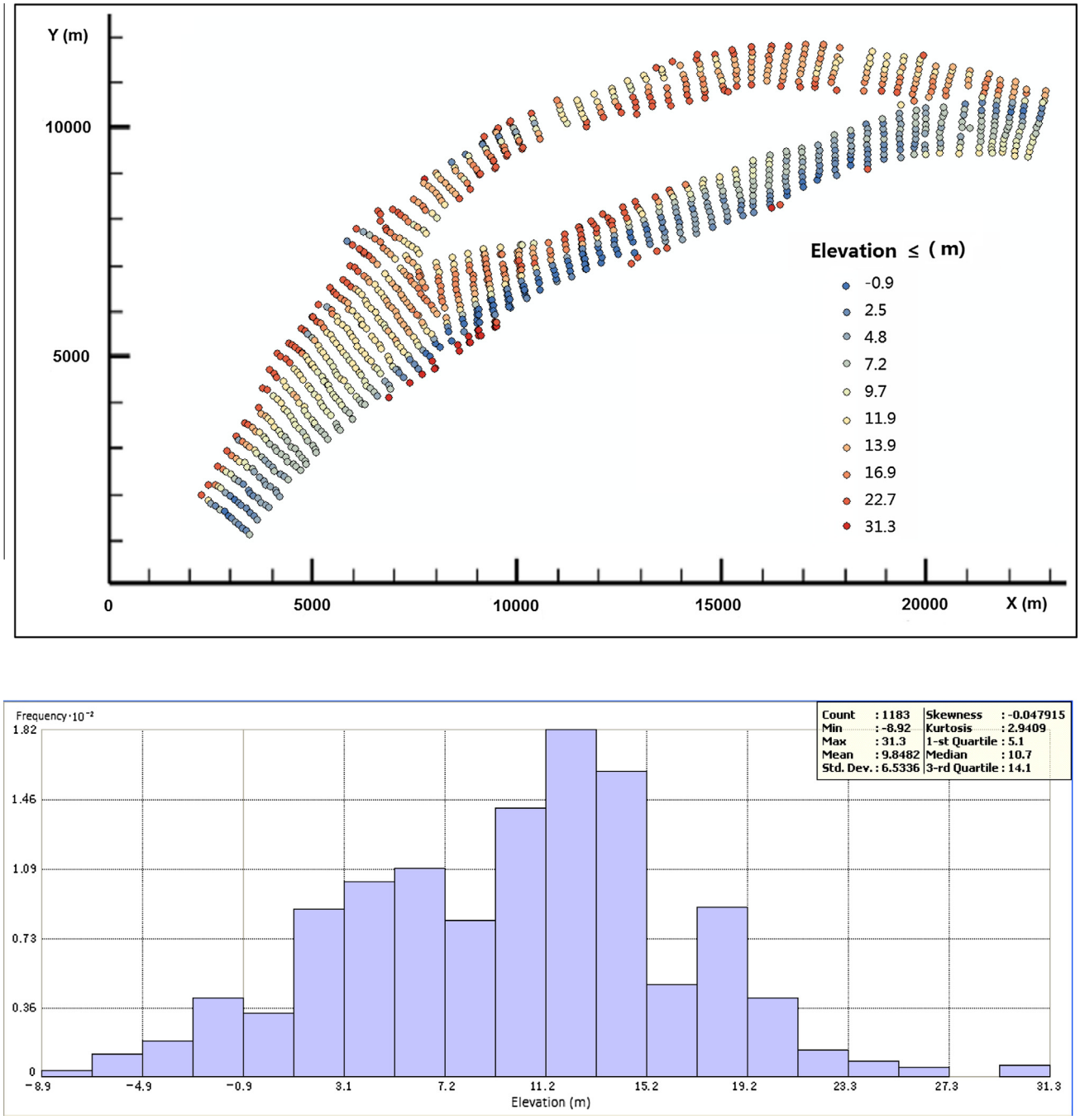

Fig. 2. The elevation and histogram of Wuhan section of Changjiang River based on 1183 samples.

two nodes. When this temporal distance is used in the interpolator, the effect of the anisotropy will significantly decrease. The corresponding shortest temporal distance method (STD) was developed through the following steps (Fig. 3).

Step 1: Generate the flow field. Based on the topography of the river channel generated by IDW (Babak and Deutsch, 2008), the flow field of river was generated by the hydrodynamic model developed in our previous studies (Zhang et al., 2012); though other models, such as Delft3D (Rinaldi et al., 2008) and Mike21 (Warren and Bach, 1992), could have also been used. The topography data generated by IDW are not very accurate but are widely used to perform hydrodynamic simulations in many studies (Ng et al., 2010).

Step 2: Calculate the temporal distance between two neighboring nodes. This is calculated by Eq. (2), whose derivation is given in Fig. 4. The TDs between all neighboring nodes are calculated in this study.

$$T_{AB} = \frac{2(\Delta x^2 + \Delta y^2)}{(u_A + u_B)\Delta x + (v_A + v_B)\Delta y} \tag{2}$$

where T_{AB} is the temporal distance between node A and its neighbor B(s); u_A and v_A are the horizontal and vertical speed of flow in the river at node A (m/s); u_B and v_B are the horizontal and vertical speed of flow in the river at node B (m/s).

Step 3: Find the shortest temporal distance from node to sample. Calculate the shortest temporal distance T_{ij} from a node (i)

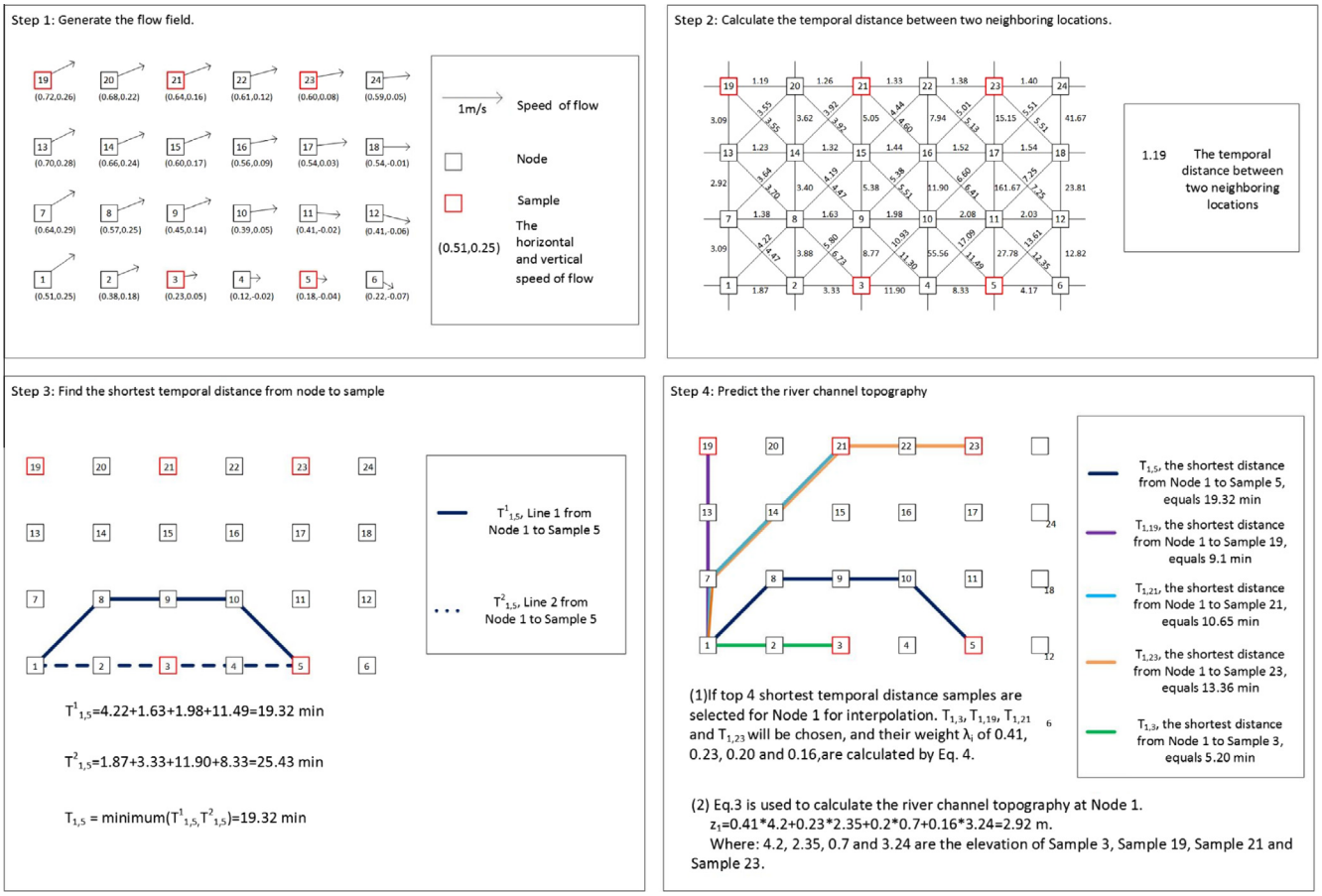

Fig. 3. The schematic figure of the shortest temporal distance method (the samples are a subset of nodes).

to a sample (j) using the Dijkstra algorithm (DIJKSTRA, 1959). The Dijkstra algorithm is an algorithm for finding the shortest paths between nodes in a weighted graph where the weighting is the inverse of TD between two neighboring nodes. Repeating the process for each pair of node and sample.

Step 4: Predict the river channel topography. The top n shortest temporal distance samples were selected for a node (i), and its topography was predicted using Eq. (3). Repeating the process for every node yields the topography of the entire river channel.

$$z^* = \sum_{i=1}^{n} \lambda_i z_i \tag{3}$$

where z^* is the predicted topography of a node (m); n represents the number of samples chosen for prediction; z_i represents the elevation sample at location i (m), and λ_i is the weight which is calculated by Eq. (4).

$$\lambda_i = \frac{1/T_i}{\sum_{i=1}^{n} 1/T_i} \tag{4}$$

where T_i is the shortest temporal distance between a node and the sample i(s).

3.2. The modified shortest temporal distance method (MSTD)

In the shortest temporal distance method mentioned above, the temporal distance between two nodes is equal to their spatial distance divided by the component of the average flow velocity along the tangent (parallel) direction of those two nodes. The normal (perpendicular) component of average velocity is neglected, which may decrease the accuracy because the normal component takes the flow away from the tangential direction, and makes the flow move along the combined direction. To improve the accuracy of the method, it may be helpful to include a penalty function in Eq. (2), and the modified temporal distance (MTD) is shown in Eq. (5). A more detailed derivation is shown in Fig. 4. If the TD calculation above is replaced by the MTD, the modified shortest temporal distance method (MSTD) is obtained.

$$T'_{AB} = \frac{2(\Delta x^2 + \Delta y^2)}{(u_A + u_B)\Delta x + (v_A + v_B)\Delta y} + P * \frac{(v_A + v_B)\Delta x - (u_A + u_B)\Delta y}{\sqrt{(\Delta x^2 + \Delta y^2)(u_{AB}^2 + v_{AB}^2)}} \tag{5}$$

where P is the penalty coefficient (s).

3.3. Inverse distance weighting (IDW) and Universal Kriging (UK)

The IDW and UK are implemented to compare the results with those obtained using STD and MSTD. IDW is a deterministic and robust interpolation method that estimates values with a weighted average of values of sample data points, with weighting factors proportional to the inverse distance. It is one of the simplest and most popular interpolation techniques (Babak and Deutsch, 2008).

Kriging is a method of interpolation which gives the best linear unbiased prediction of the intermediate values, and is widely used in the spatial analysis. Ordinary Kriging (OK) assumes the constant mean is unknown, and is the most generally used of the Kriging methods. UK assumes a general polynomial trend model which is

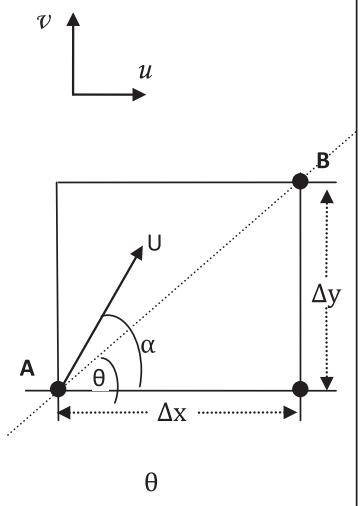

Time (Temporal Distance) from A to B

(a): Calculate the average speed U along the direction A-B

$$u_{AB} = \frac{u_A + u_B}{2} \quad v_{AB} = \frac{v_A + v_B}{2}$$

(b): Calculate the trigonometric functions

$$cos\alpha = \frac{u_{AB}}{\sqrt{u_{AB}^2 + v_{AB}^2}} \quad sin\alpha = \frac{v_{AB}}{\sqrt{u_{AB}^2 + v_{AB}^2}}$$

$$cos\theta = \frac{\Delta x}{\sqrt{\Delta x^2 + \Delta y^2}} \quad sin\theta = \frac{\Delta y}{\sqrt{\Delta x^2 + \Delta y^2}}$$

$$\cos(\alpha - \theta) = cos\alpha cos\theta + sin\alpha sin\theta$$

where α is the angle between flow velocity and horizontal direction; θ is the angle between A-B direction and horizontal direction.

(c): Calculate the time from A to B

$$T_{AB} = \frac{Distance}{Speed} = \frac{\sqrt{\Delta x^2 + \Delta y^2}}{\sqrt{u_{AB}^2 + v_{AB}^2}\cos(\alpha - \theta)} = \frac{2(\Delta x^2 + \Delta y^2)}{(u_A + u_B)\Delta x + (v_A + v_B)\Delta y}$$

d): Calculate the modified time from A to B by introducing the penalty function (P)

$$T'_{AB} = \frac{Distance}{Speed} + T_p = \frac{2(\Delta x^2 + \Delta y^2)}{(u_A + u_B)\Delta x + (v_A + v_B)\Delta y} + P * sin(\alpha - \theta)$$

$$= \frac{2(\Delta x^2 + \Delta y^2)}{(u_A + u_B)\Delta x + (v_A + v_B)\Delta y} + P * \frac{(v_A + v_B)\Delta x - (u_A + u_B)\Delta y}{\sqrt{(\Delta x^2 + \Delta y^2)(u_{AB}^2 + v_{AB}^2)}}$$

Fig. 4. Steps of calculating temporal distance between neighboring nodes.

used to remove the trend from the data by subtracting it from the original measured point (Goovaerts, 1997). Once the model is fit to the random errors, the polynomial is added back to the predictions to give meaningful results. Due to the obvious trend in the topography of a river channel that goes along with thalweg, the trend obtained by UK with first- or second-order polynomials is a better choice than the trend obtained with Ordinary Kriging (Legleiter and Kyriakidis, 2008).

The IDW and UK are carried out by the Geostatistics Analyst tool of ArcGIS 9.3.

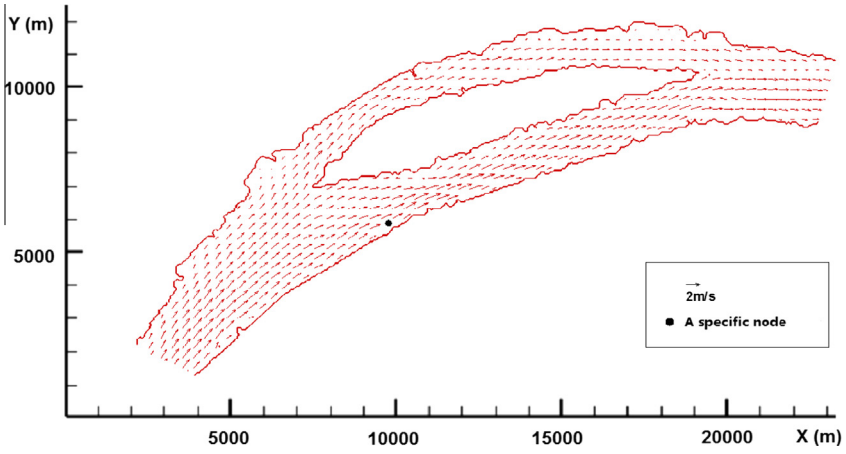

Fig. 5. The flow field of the Wuhan section of the Changjiang River. The specific node (X = 10,000 m, Y = 5800 m; black point) is chosen for comparing the spatial distances and the temporal distances in Fig. 6.

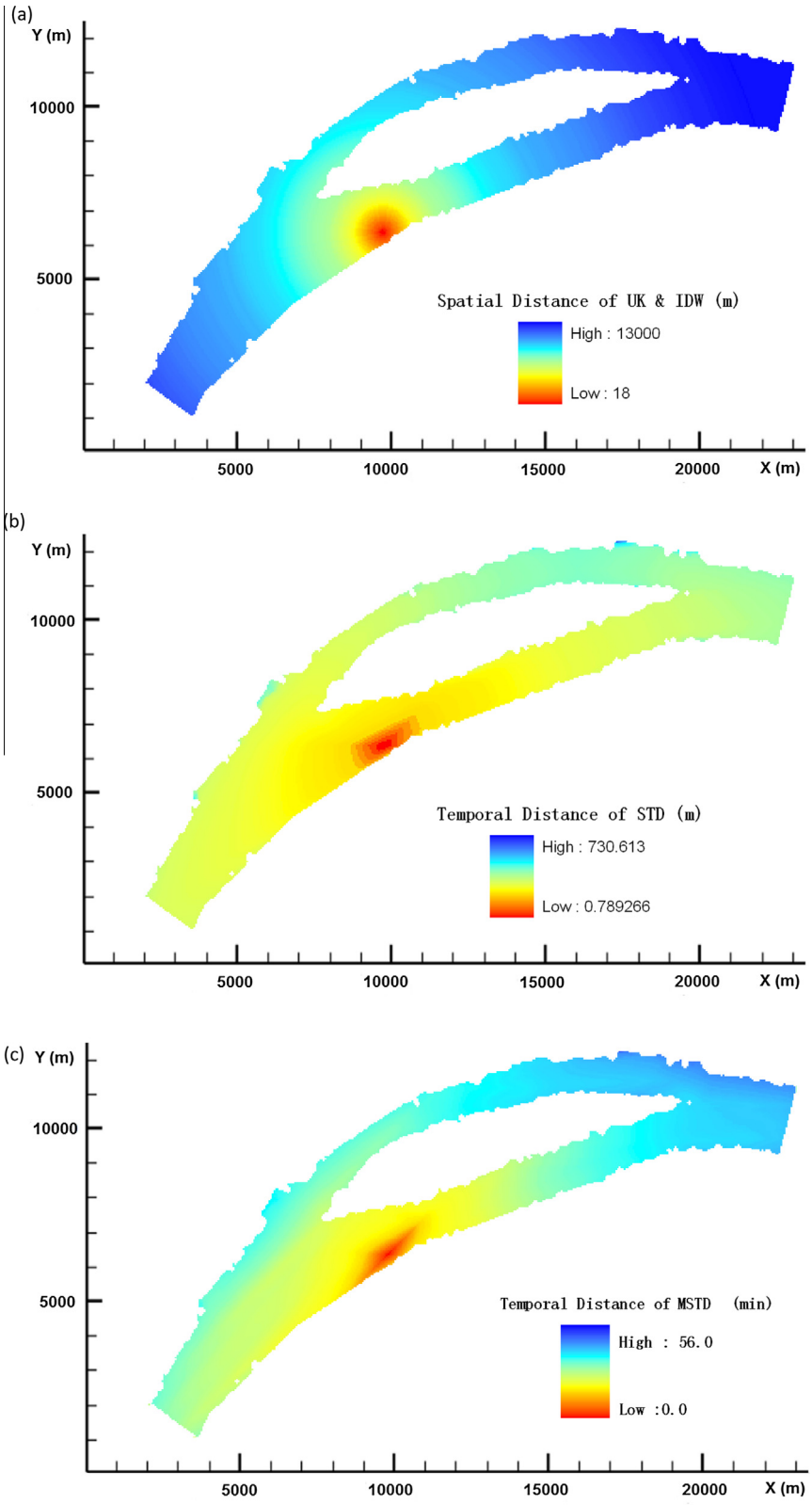

Fig. 6. The spatial distances and temporal distances from the node (X = 10,000 m, Y = 5800 m) to the other nodes. ((a) The spatial distance used in IDW and UK; (b) the temporal distance used in STD is approximately in accordance with the flow; (c) the modified temporal distance used in MSTD is accurately in accordance with the flow direction.)

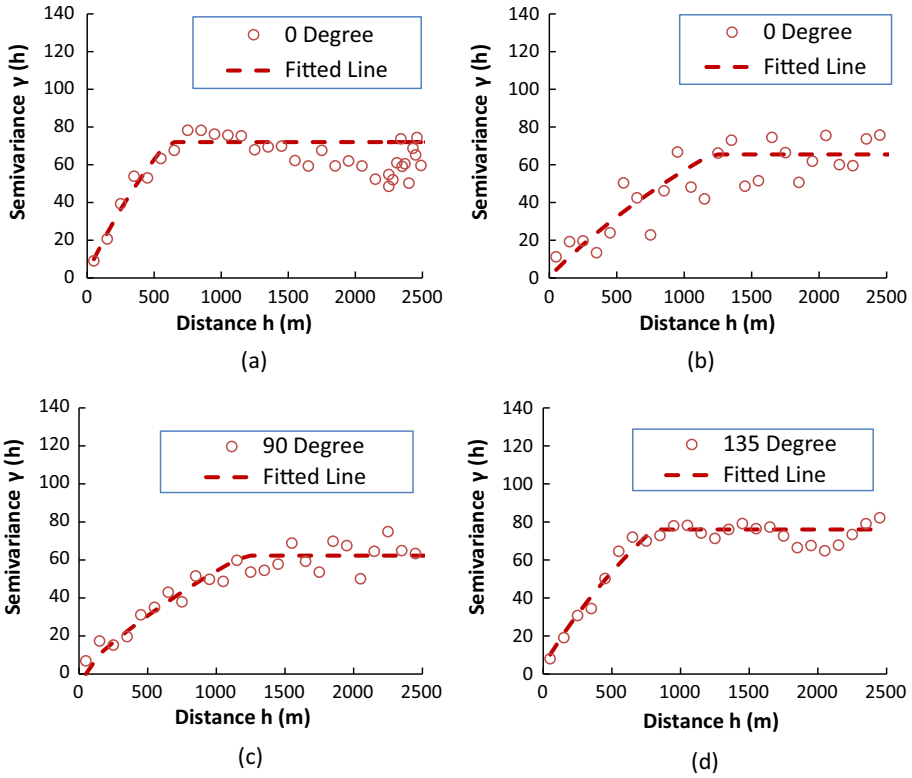

Fig. 7. The semivariograms of river channel topography in different azimuths (0°, 45°, 90°, 135°). As both the range and sill varied with the direction of the semivariogram, it obviously represents zonal anisotropy.

4. Results

4.1. Generation of flow field

Based on the topography of the river channel interpolated by IDW using ArcGIS, a DEM-based hydrodynamic model was used to generate the flow field and had been validated in our previous study (Zhang et al., 2012). The flow field of the Wuhan section of the Changjiang River is shown in Fig. 5 and was used in the STD and MSTD analysis.

4.2. Calculating the spatial distance and temporal distance

Based on the flow field, the SD, TD and MTD between nodes were calculated by Eqs. (1), (2) and (5). Using the node (X = 10,000 m, Y = 5800 m) as an example, the SD field from each node of the grid to that specific node is shown in Fig. 6a. The SDs presents an obvious circle that is independent of the flow field shown in Fig. 5. Therefore, the interpolator based on SD would give a poor prediction of river channel topography. The TDs presents a rectangle, which is approximately in accordance with the flow (Fig. 6b); and the MSD presents a diamond, which is more accurately in accordance with the flow direction (Fig. 6c).

4.3. Semivariogram

A semivariogram is one of the significant functions to indicate spatial correlation in observations measured at sample locations. It is often calculated by Eq. (6) in Kriging (Legleiter and Kyriakidis, 2008).

$$\gamma(h) = \frac{1}{2N_h}\sum_{i=1}^{N_h}(z_i - z_{i+h})^2 \quad (6)$$

where Z_i is the elevation of sample at location i (m); Z_{i+h} is the elevation of another sample at a distance h from i (m); and N_h is the number of data pairs at a distance h.

The semivariogram of the study area was calculated by Eq. (6), and the semivariogram and their fitted models in four typical azimuths (0°, 45°, 90°, and 135°) with bandwidth 300 m and angle tolerance 45°, are shown in Fig. 7. As both the range and sill varied with the direction of the semivariogram, it is the zonal anisotropy (sill anisotropy) which is the common type of anisotropy. Such a structure is difficult to transform into an isotropic semivariogram. For zonal anisotropy, sill is an important parameter to determine the magnitude of anisotropy. In these four directions, both sills of the fitted spherical models in 45° and 90° are less than 66 m^2, and the sills in 0° and 135° are greater than 72 m^2. After multiple trials, the major azimuth (66°) reflecting the prominent directionality along the channel was found, and a spherical model was chosen to fit the empirical semivariogram (Fig. 8a). Its sill is 55.3 m^2, which is less than sills of the other directions.

To illustrate the performance in decreasing the effect of anisotropy, the semivariogram of TD and MTD was calculated and compared to the one obtained with the spatial distance. As the temporal distance is introduced to replace the spatial distance, the semivariogram is calculated by Eq. (7).

$$\gamma(t) = \frac{1}{2N_t}\sum_{i=1}^{N_t}(z_i - z_{i+t})^2 \quad (7)$$

where Z_i is the elevation of sample at location i (m); Z_{i+t} is the elevation of another sample taken t intervals away from i (m); and N_t is the number of pairs of data at a temporal distance t.

The result is shown in Fig. 8b and c. As the different method uses a different distance metric, the ranges cannot be compared and sill may be the best available parameters to represent the level of anisotropy. Similar to the result presented by Legleiter and

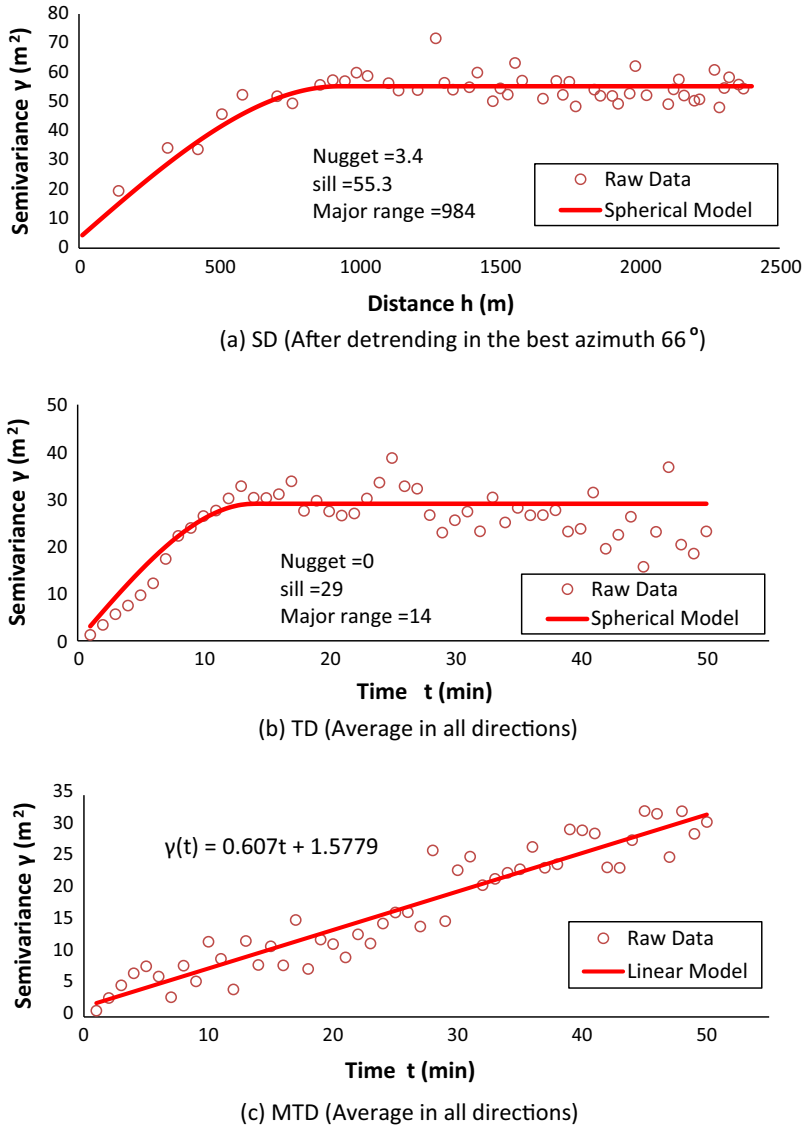

Fig. 8. Semivariogram model (line) and its original data (point). The result of compared Sill showed TD may indicate less anisotropy than SD. Though the semivariogram model of MTD cannot be compared with SD and TD, it is obvious that the semivariance of MTD is smaller than TD, especially when only several close samples are used in prediction.

Kyriakidis (2008) and Boisvert and Deutsch (2011a), smaller sill often meant a much stronger spatial correlation in observations measured at sample locations. The sill of TD which obeys the spherical model is 29 m^2, which is much less than that of Kriging (55.3 m^2). So the TD may be better than the SD in modeling the topography of a river channel with stronger anisotropy. Additionally, though the linear semivariogram model of MTD cannot be compared with the spherical one, the semivariance of MTD is less than that of TD, especially when only several close samples are used in prediction. It implies MSTD may give better performance than STD.

4.4. Interpolation of river channel topography

The topography of the river channel at the Wuhan section of Changjiang River has been interpolated using the IDW, UK, STD and MSTD independently following the previous steps. A second order polynomial trend surface was fitted in UK. The major direction of UK is 66°, and the spherical model is chosen as the semivariogram model which is shown in Fig. 8a. The STD and MSTD were coded using Matlab. The n of 8 and the penalty coefficient (P) of MSTD of 32 s were selected after multiple trials between the range of the 1st and 19th 20-quantile of STD. All the results are shown in Fig. 9.

The topography generated by IDW has many bumps and jaggies, and the thalweg of river in the lower branch is not continuous. Clearly this method does not capture the prevailing trend of river channel topography and the prediction is not accurate (Fig. 9a).

The UK (Fig. 9b), the STD (Fig. 9c) and the MSTD (Fig. 9d) have few jaggies, and the obvious and continuous thalweg in their prediction maps indicate a more realistic captured prevailing trend. In these results, the UK has many unreasonable strips (Fig. 9b), which suggests that the UK had over-fitted the river channel topography. Meanwhile, the STD and MSTD both yielded a smooth simulation despite the local anisotropy (Fig. 9c and d).

4.5. Cross validation

To compare the performance of these methods quantitatively, leave-one-out cross validation was adopted for all of the 1183

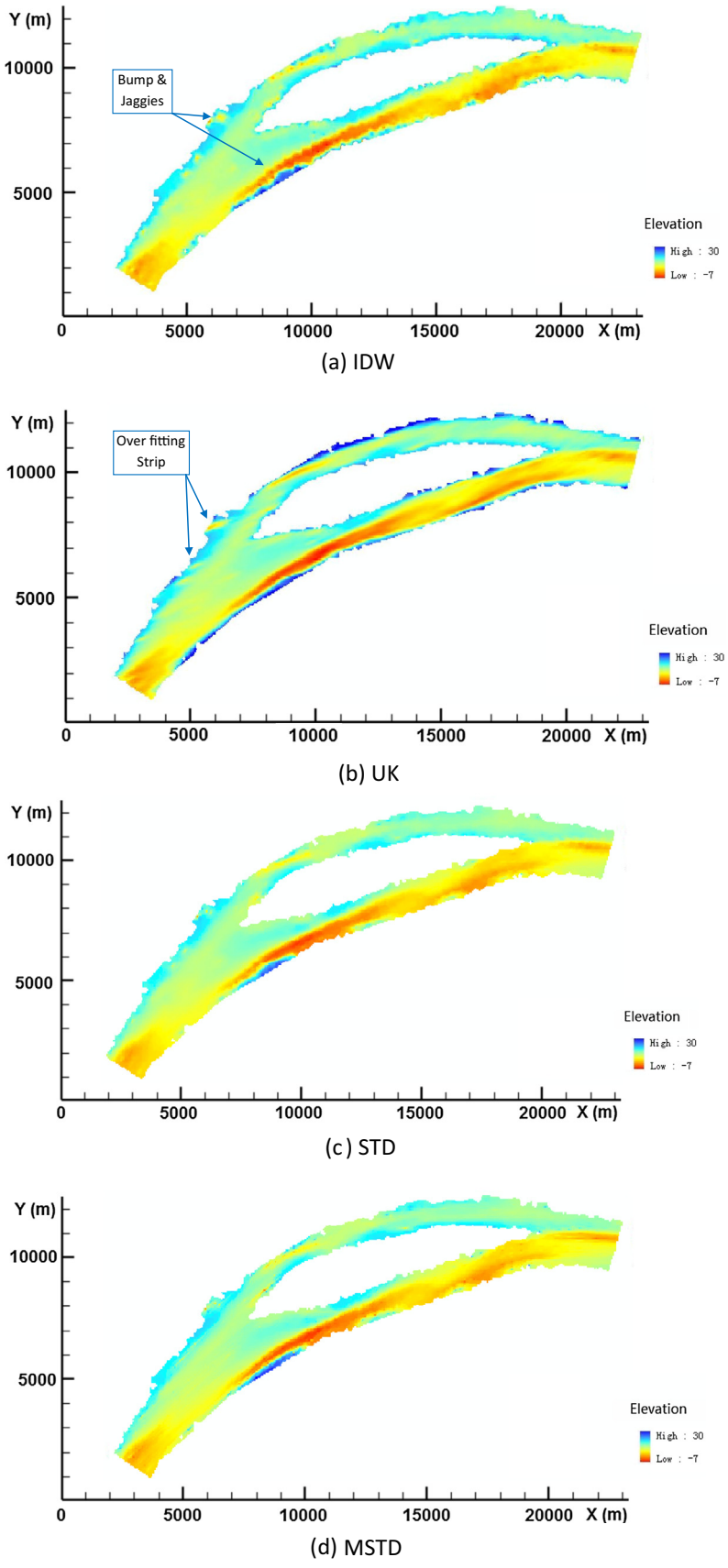

Fig. 9. Topography prediction of the Wuhan section of the Changjiang River by different methods. IDW has a lot of bumps and jaggies. The UK has a lot of unreasonable strips due to its unsuitable semivariance model to estimate the anisotropy. The STD and MSTD both yield a smooth simulation despite the local anisotropy.

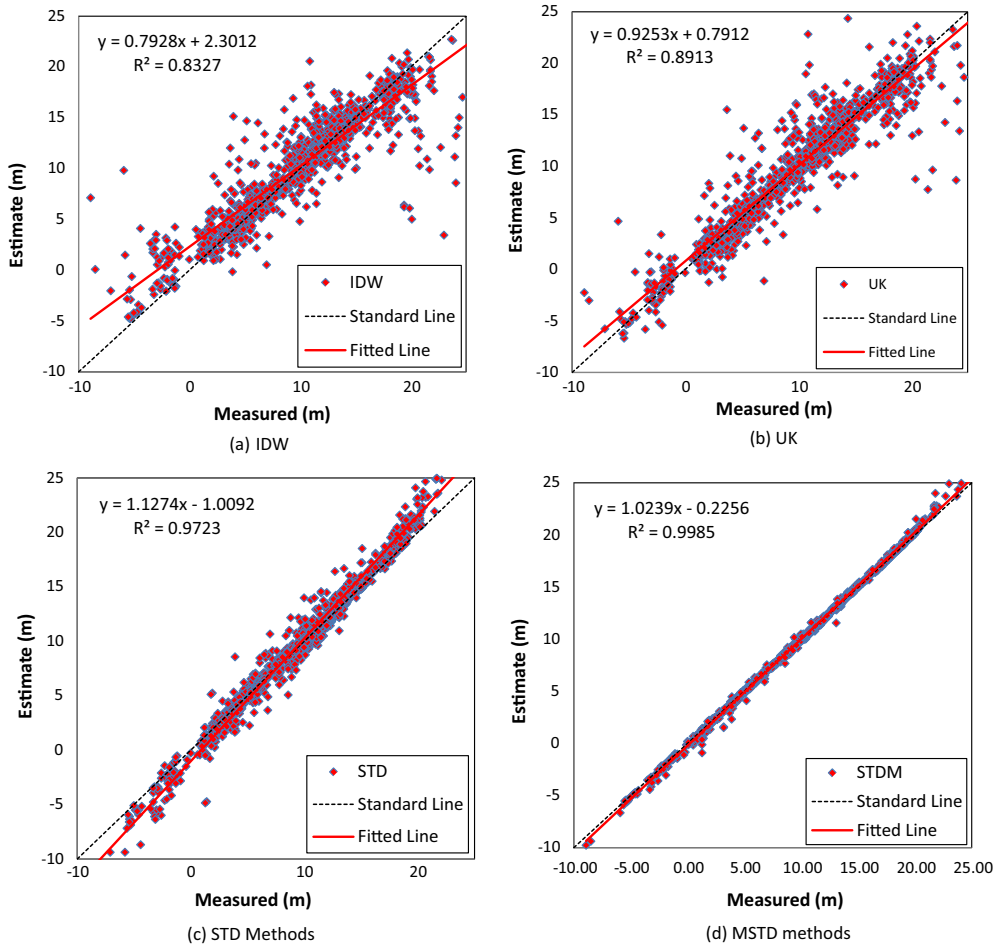

Fig. 10. The comparisons of measured and estimated values for each point by the 4 methods.

samples. The predicted elevations over the measured elevations are shown in Fig. 10 with a fitted line. The coefficients of determination (R^2), slopes and intercepts are compared comprehensively in Fig. 10, and indicate that the MSTD performed best, followed by STD, IDW, and UK.

Beyond coefficient of determination, three other comparison criteria are analyzed. The absolute error (AE), the mean absolute percentage error (MAPE), the mean absolute error (MAE) and the mean squared error (MSE) are included (Li et al., 2014). The AE is a measure of the difference between a measurement and a true value in a node. MAPE gives an overall estimate of prediction accuracy and is scale independent (Kim and Kim, 2016). The MAE is used to quantify how close forecasts or predictions are to the observations. The MSE gives the average squared difference between the measured elevation and the estimate elevation, and incorporates both the variance of the estimator and its bias.

The results of AE are shown in Fig. 11. Based on these maps, the ranking of methods in AE is MSTD > STD > UK > IDW. The results of the other criteria are shown in Table 1, which shows that the MSTD yielded the best performance in all the four comparison criteria, followed by the STD. These statistics also show that the MSTD and STD yield remarkable improvements in the prediction accuracy compared to the more widely used methods. Based on the theory of sediment transport, the topography of a river channel is determined by both flow and geologic-tectonic features (which are mainly reshaped by the flow), and the shortest temporal distance metric could obviously improve the performance of a topography interpolator.

The UK is better in MAPE, MSE and MAE than the IDW. It is reasonable since UK is complicated and designed to account for anisotropy. However, UK also performed worse than STD and MSTD, as the strong effect of anisotropy of a river channel is difficult to decrease by selecting a suitable covariance function in UK.

5. Discussion

As the flow field is an important factor for deposition and erosion of river bed sediment, it is reasonable to incorporate it into an interpolator of topography of river channels. In this study, STD and MSTD metrics estimated by flow velocity are developed. The potential for improving the performance of topography interpolator is demonstrated.

For the STD and MSTD, the flow field is first calculated by hydrodynamic equations. The flow field calculation is often complex, however, most researchers who need the topography of a river channel are able to calculate the flow field using their own models or readily-available models such as MIKE21 (Warren and Bach, 1992), or Delft3D (Rinaldi et al., 2008). In many studies, the flow field simulation is the next target after topography prediction. Calculating the river channel topography using STD is computationally intensive. At the current stage of development without algorithm optimization, doing the computation in Matlab requires approximately 1 h. Because this study focused mainly on improving and validating the effectiveness of the proposed methods, rather than improving the efficiency of method and decreasing

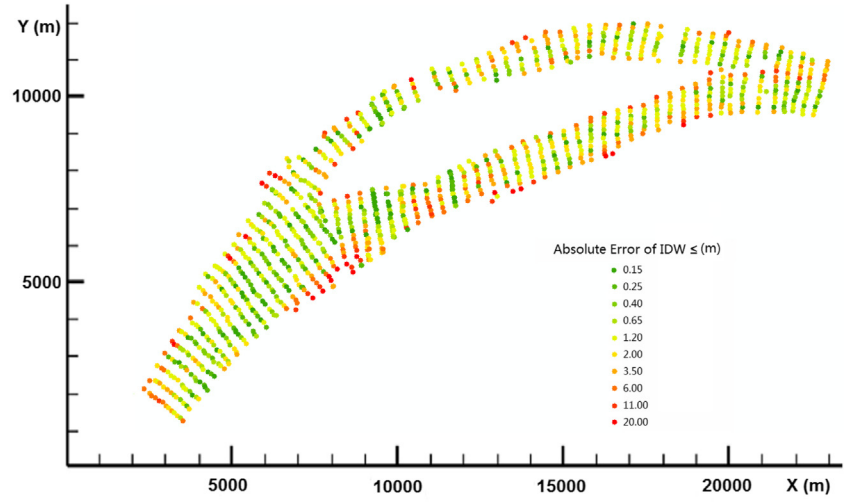

(a) IDW

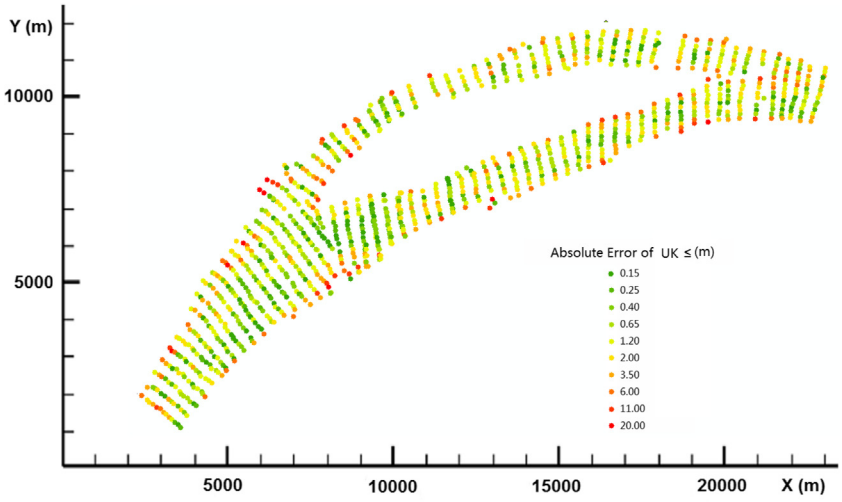

(b) UK

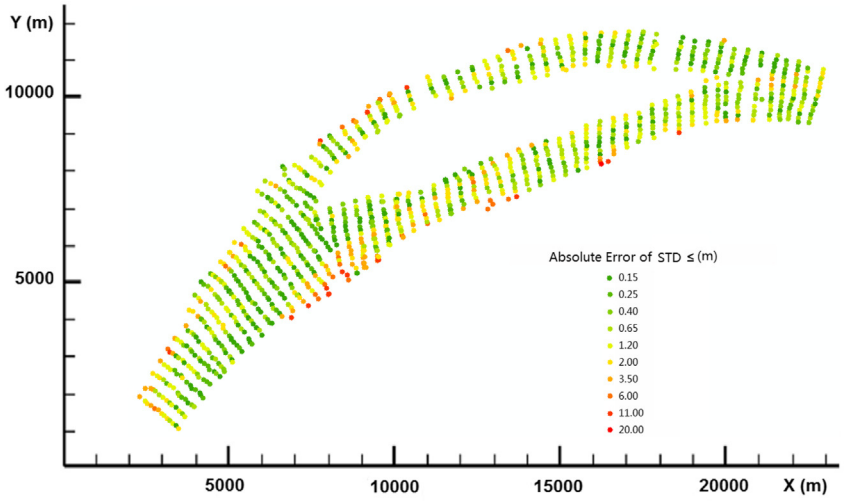

(c) STD

Fig. 11. The absolute error (AE) of cross validation. Based on the four panels, the ranking in AE is MSTD > STD > UK > IDW.

the computation time, optimizing computational efficiency will be an important area for further development.

The inaccuracies of topography generated by the IDW may propagate to the flow field, and then to the topography generated by STD

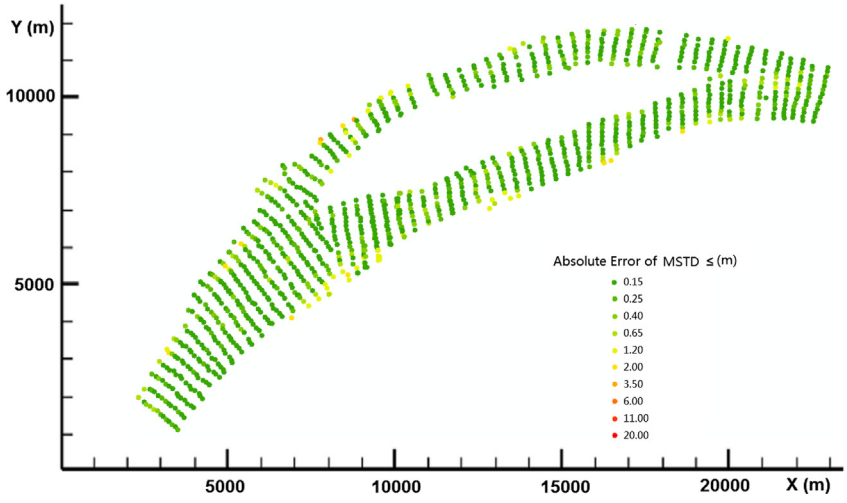

(d) MSTD

Fig. 11 (*continued*)

Table 1
The comparisons of accuracy of the four interpolation methods.

Comparison criteria	Measured samples	IDW	UK	STD	MSTD
Mean (m)	9.84	10.04	9.91	10.03	9.85
Standard deviation (m)	6.53	5.55	6.26	7.27	6.58
MAE (m)		1.55	1.26	0.82	0.16
MSE (m^2)		6.94	4.49	2.03	0.08
MAPE		26.08%	18.67%	13.11%	4.34%
R^2		0.8327	0.8913	0.9723	0.9985

and MSTD. But the accuracy of hydrodynamic model is only slightly sensitive to the topography (Horritt et al., 2006). Therefore, the inaccuracies of the topography do not significantly impact the results of STD and MSTD. The accuracy of STD and MSTD is much better than IDW, and it implies the inaccuracy of IDW propagated to STD and MSTD will be decreased. It is worth discussing how much the results of STD and MSTD are dependent on a good initial topography and a good flow simulation, and further improve the STD and MSTD. We expect that future studies will demonstrate this point.

Additionally, UK is used to compare with STD and MSTD in this study and shows a worse performance. Theoretically, UK should yield satisfactory performance as an overriding trend is assumed and modeled by a deterministic function in the interpolation. However, in conditions where the trend is extremely difficult to fit to a polynomial, UK will yield inaccuracies in the predicted topography. Some techniques such as element-by-element piecewise kriging (Wong and Kanok-Nukulchai, 2009) and the kriging using local anisotropies (Soares, 1992) may improve the accuracy of kriging on the river channel, and further investigation of such improvements are an important area for future study.

6. Conclusions

Two major conclusions can be drawn from this study:

(1) The anisotropy of topography of a river channel is often the result of hydrodynamic or transport mechanisms, and the principal axes of the anisotropy are determined by the direction of flow (Kitanidis, 1997). Therefore, the shortest temporal distance metric estimated by flow velocity can be adopted to replace the spatial distance (Euclidean distance) metric in a spatial interpolator.

(2) The STD and MSTD have a better performance than the IDW and UK in the river sections studied. Furthermore, the MSTD has the best potential for predicting the river channel topography based on the temporal distance metric.

Acknowledgement

This study was funded by the National Natural Science Foundation of China under Grants 51209162 & 51379149, the Major Science and Technology Program for Water Pollution Control and Treatment of China under Gant 2014ZX07104-005, and the China Scholarship Council under Grant 201406275007.

Appendix A. Supplementary material

Supplementary data associated with this article can be found, in the online version, at http://dx.doi.org/10.1016/j.jhydrol.2016.09.022. These data include Google maps of the most important areas described in this article.

References

Babak, O., Deutsch, C.V., 2008. Statistical approach to inverse distance interpolation. Stochastic Environ. Res. Risk Assess. 23 (5), 543–553. http://dx.doi.org/10.1007/s00477-008-0226-6.

Boisvert, J.B., Deutsch, C.V., 2011a. Modeling locally varying anisotropy of CO_2 emissions in the United States. Stochastic Environ. Res. Risk Assess. 25 (8), 1077–1084. http://dx.doi.org/10.1007/s00477-011-0483-7.

Boisvert, J.B., Deutsch, C.V., 2011b. Programs for kriging and sequential Gaussian simulation with locally varying anisotropy using non-Euclidean distances. Comput. Geosci. 37 (4), 495–510. http://dx.doi.org/10.1016/j.cageo.2010.03.021.

DIJKSTRA, E., 1959. A note on two problems in connexion with graphs. Numer. Math. 1, 269–271.

Gardner, B., Sullivan, P.J., Lembo, J.A.J., 2003. Predicting stream temperatures: geostatistical model comparison using alternative distance metrics. Can. J. Fisheries Aquatic Sci. 60 (3), 344–351. http://dx.doi.org/10.1139/f03-025.

Goovaerts, P., 1997. Geostatistics for Natural Resources Evaluation. Oxford University Press.

Harvey, J.W., Bencala, K.E., 1993. The effect of streambed topography on surface-subsurface water exchange in mountain catchments. Water Resour. Res. 29 (1), 89–98. http://dx.doi.org/10.1029/92WR01960.

Hoef, J.M.V., Peterson, E., Theobald, D., 2006. Spatial statistical models that use flow and stream distance. Environ. Ecol. Statist. 13 (4), 449–464. http://dx.doi.org/10.1007/s10651-006-0022-8.

Horritt, M.S., Bates, P.D., Mattinson, M.J., 2006. Effects of mesh resolution and topographic representation in 2D finite volume models of shallow water fluvial flow. J. Hydrol. 329 (1–2), 306–314.

Kim, S., Kim, H., 2016. A new metric of absolute percentage error for intermittent demand forecasts. Int. J. Forecasting 32 (3), 668–679.
Kitanidis, P., 1997. Introduction to Geostatistics: Applications in Hydrogeology. Cambridge University Press.
Legleiter, C.J., Kyriakidis, P.C., 2008. Spatial prediction of river channel topography by kriging. Earth Surf. Processes Landforms 33 (6), 841–867. http://dx.doi.org/10.1002/esp.1579.
Li, L., Gong, J., Zhou, J., 2014. Spatial interpolation of fine particulate matter concentrations using the shortest wind-field path distance. PloS one 9 (5), e96111. http://dx.doi.org/10.1371/journal.pone.0096111.
Marzadri, A., Tonina, D., Bellin, A., Tank, J.L., 2014. A hydrologic model demonstrates nitrous oxide emissions depend on streambed morphology. Geophys. Res. Lett. 41 (15), 5484–5491.
Mejia, A., Reed, S., 2011. Role of channel and floodplain cross-section geometry in the basin response. Water Resour. Res. 47 (9), W09518. http://dx.doi.org/10.1029/2010WR010375.
Merwade, V., 2009. Effect of spatial trends on interpolation of river bathymetry. J. Hydrol. 371 (1–4), 169–181. http://dx.doi.org/10.1016/j.jhydrol.2009.03.026.
Ng, S.M.N., Wai, O.W.H., Xu, Z.H., Li, Y.S., 2010. Integrating GIS with Hydrodynamic Model for Wastewater Disposal and Management: Pearl River Estuary. 13, pp. 207–217. http://dx.doi.org/10.1007/978-1-4020-9720-1_19.
Rinaldi, M., Mengoni, B., Luppi, L., Darby, S.E., Mosselman, E., 2008. Numerical simulation of hydrodynamics and bank erosion in a river bend. Water Resour. Res. 44 (9).
Rivest, M., Marcotte, D., Pasquier, P., 2012. Sparse data integration for the interpolation of concentration measurements using kriging in natural coordinates. J. Hydrol. 416–417, 72–82. http://dx.doi.org/10.1016/j.jhydrol.2011.11.043.
Schwendel, A.C., Fuller, I.C., Death, R.G., 2012. Assessing DEM interpolation methods for effective representation of upland stream morphology for rapid appraisal of bed stability. River Res. Appl. 28 (5), 567–584. http://dx.doi.org/10.1002/rra.1475.
Shope, C., Constantz, J., Cooper, C., Reeves, D., Pohll, G., McKay, W., 2012. Influence of a large fluvial island, streambed, and stream bank on surface water-groundwater fluxes and water table dynamics. Water Resour. Res. 48 (6), W06512. http://dx.doi.org/10.1029/2011WR011564.
Soares, C., 1992. Geostatistical estimation of multi-phase structures. Math. Geol. 24 (2), 149–160.
Warren, I.R., Bach, H., 1992. MIKE 21: a modelling system for estuaries, coastal waters and seas. Environ. Software 7 (4), 229–240.
Wildhaber, Y.S., Michel, C., Epting, J., Wildhaber, R.A., Huber, E., Huggenberger, P., Alewell, C., 2014. Effects of river morphology, hydraulic gradients, and sediment deposition on water exchange and oxygen dynamics in salmonid redds. Sci. Total Environ. 470, 488–500.
Wong, F., Kanok-Nukulchai, W., 2009. Kriging-based finite element method: element-by-element Kriging interpolation. Civ. Eng. Dimension 11 (1), 15–22.
Zhang, Y.J., Jha, M., Gu, R., Wensheng, L., Alin, L., 2012. A DEM-based parallel computing hydrodynamic and transport model. River Res. Appl. 28 (5), 647–658. http://dx.doi.org/10.1002/rra.1471.